Available online at www.sciencedirect.com

ScienceDirect

Solar Energy 118 (2015) 186–196

SOLAR ENERGY

www.elsevier.com/locate/solener

Building shape optimisation to reduce air-conditioning needs using constrained evolutionary algorithms

Gianpiero Caruso [a,*], Jérôme Henri Kämpf [b]

[a] Department of Energy and System Engineering (DESE), University of Pisa, Largo Lucio Lazzarino, I-56126 Pisa, Italy
[b] Solar Energy and Building Physics Laboratory, Station 18, École Polytechnique Fédérale de Lausanne, 1015 Lausanne, Switzerland

Received 16 November 2014; received in revised form 8 April 2015; accepted 28 April 2015
Available online 9 June 2015

Communicated by: Associate Editor Mario A. Medina

Abstract

The purpose of this paper is to analyse the optimal three-dimensional form of buildings that minimise energy consumption due to solar irradiation. We use an evolutionary algorithm (hybrid CMA-ES/HDE algorithm) already applied to maximise solar energy utilisation (Kämpf and Robinson, 2010), which uses a cumulative sky model approach for the computation of incident irradiation on the building envelope.

Various families of possible building forms are investigated with this methodology to find the optimal building form, in two locations with radically different climatic conditions, showing the features that a building should posses in order to optimise its energy performance with respect to the solar irradiation.

Keywords: Building form optimisation; Constrained evolutionary algorithms; Point of maximum algebraic/cumulated solar irradiation; Hybrid CMA-ES/HDE algorithm

1. Introduction

In building facing particularly hot climatic conditions, the greatest source of internal gains is solar radiation. This radiation can enter buildings directly through windows or it can heat the building shell to a higher temperature than the ambient one, increasing the heat transfer through the building envelope. As a result, the electricity consumption due to the air-conditioning (AC) in summer is a relevant problem in various warm and temperate climate regions. E.g. the annual electricity peak power in Italy is reached in summer for the first time in recent years and is increasing in intensity, probably due to an increasing diffusion of AC for the summer cooling of buildings (Terna s.p.a).

Solar gain can be reduced by adequate shading from the sun, light coloured roofing, spectrally selective (heat-reflective) paints and coatings and various types of insulation for the rest of the envelope. However, these solutions reduce in general interior daylighting, increasing energy consumption due to artificial lighting.

Another approach is to optimise the global form of the building envelope to reduce energy consumption due to solar irradiation. The problem of building's form optimisation has been investigated in many publications with an analytical approach based on variational methods (Caruso et al., 2013), and with a numerical approach by using multicriteria optimisation (Marks, 1997; Farmani

* Corresponding author. Tel.: +39 389 97 58 253.
E-mail address: gianpi.caruso@gmail.com (G. Caruso).

http://dx.doi.org/10.1016/j.solener.2015.04.046
0038-092X/

Nomenclature

$\vec{L}$, L	the radiance distribution in the cumulative sky
$\dot{L}$	the normalised radiance distribution in the cumulative sky
$\vec{L}_i$	the radiance on the ith Tregenza patch
I	the total solar irradiation on a surface
r	the ratio of the direct solar radiation contribute to the total radiation
$\hat{n}(\sigma,\psi)$	the normal vector of a given surface
σ, Σ	the tilt angle of a given surface, i.e. the angle between the surface and the vertical
ψ	the orientation of a given surface (zero to the South and positive to the West)
θ	the zenith angle defining the position in the cumulative sky of a radiant source
ϕ	the azimuth angle defining the position in the cumulative sky of a radiant source (zero to the South and positive to the West)
φ	the day angle
θ	the solar zenith angle
δ	the declination
L	the latitude
ω	the hour angle
$\mathbb{R}$	the set of real numbers
$\mathbb{R}^+$	the set of positive real numbers
$\mathcal{B}$	a Banach space
$\mathcal{D}$	a space of distributions
λ	the wavelength
$H_{0\lambda}$	the extraterrestrial spectral irradiance at the mean solar distance
D	the correction factor for the earth–sun distance
$T_{r\lambda}$	the transmittance function for Rayleigh scattering
$T_{a\lambda}$	the transmittance function for aerosol extinction
$T_{0\lambda}$	the transmittance function for ozone absorption
$T_{w\lambda}$	the transmittance function for water vapour absorption
$T_{u\lambda}$	the transmittance function for absorption by the uniformly mixed gases (oxygen and carbon dioxide)
$a_{0,\lambda}$	the ozone absorption coefficients
$a_{w,\lambda}$	the water vapour and mixed gas absorption coefficients
$a_{u,\lambda}$	the mixed gas absorption coefficients
W_0	the single scattering albedo of the aerosol
F_a	the forward to total scattering ratio of the aerosol
T_e	the external temperature
T_c	the internal comfort temperature

Superscripts

$^{(v)}$	refers to the visible spectrum

Subscripts

$_d$	refers to the direct solar radiation
$_s$	refers to the diffuse solar radiation

et al., 2002), genetic algorithms (Farmani et al., 2002; Rivard et al., 2006; Tuhus-Dubrow and Krarti, 2010; Kampf and Robinson, 2009, 2010; Kampf et al., 2010), discrete polyoptimisation (Jedrzejuk and Marks, 2002) and hierarchical geometry relations (Yi and Malkawi, 2009). In particular Kämpf and Robinson developed a method based on genetic algorithms to find the 3-dimensional form that maximises solar energy utilisation (Kampf and Robinson, 2009, 2010; Kampf et al., 2010).

In this paper, we use a numerical method and, in particular, an hybrid evolutionary algorithm developed in Kampf and Robinson (2009) and applied to optimise building geometric form for solar radiation utilisation (Kampf et al., 2010; Kampf and Robinson, 2010). We discuss the validity of the method used and exhibit optimal individuals of some parametrisation of the building's shape and associated results. Moreover a new algebraic cumulative sky is introduced in order to estimate the energy consumption due to solar gains. We conclude by extrapolating the shape that a building form should follow in order to optimise its energy consumption by a suitable solar exposure.

2. Methodology

The methodology consists in using weather data and RADIANCE (Larson and Shakespeare, 1998) in order to build the virtual scene representing the annual solar energy source of algebraic radiation on the building, i.e. considering in which case the solar irradiation on the envelope gives a positive or negative contribution depending on the external temperature. The contribution is further associated to the data of the solar irradiation for each hour of a typical year. The algebraic cumulative sky constructed on that basis has the advantage to present particular zones where the solar radiation is useful all year long.

Finally we use an hybrid evolutionary algorithm (CMA-ES/HDE algorithm) to explore the optimal building forms minimising the annual air-conditioning energy consumption.

2.1. Solar potential determination

The backward ray tracing program RADIANCE is used, in order to measure the solar potential of

hypothetical buildings. As done by Kampf and Robinson (2010), a virtual scene is defined by a sky, buildings and a ground. In order to compute the irradiation on buildings over an average year, a cumulative sky is produced for the location (Robinson and Stone, 2004). In this study, we have taken two locations to be Basel in Switzerland (47°N, 7°E) and Dubai (25°N, 55°E) and the corresponding meteorological data from the Meteonorm software (www.meteonorm.com). The virtual sky is composed of 145 Tregenza patches with corresponding cumulative radiance (W h m^{-2} s r^{-1}), as shown in Fig. 1.

The RADIANCE software is then used to determine the irradiation on surfaces that composes the virtual scene. To realise this, each surface is fitted with virtual watthour-metres in order to compute their irradiation. The total irradiation on the building form is computed by summing over all the surfaces.

2.2. Validation of the method

The irradiation on buildings is calculated using RADIANCE. This is a suite of tools for performing lighting simulation, through the red, green and blue channels in visible spectrum. So, in order to validate this method, we show that neglecting the infrared and ultraviolet does not lead to a significant error.

The problem of optimising the building form is a scalable problem, i.e. if we multiply for a factor the radiance of each Tregenza patch, the problem does not change because this is equivalent to multiply by the same factor the objective function. Hence, from the point of view of the radiation sources, the problem is completely defined by the radiance distribution in the cumulative sky, $\vec{\beth}$, that allows to calculate the total solar irradiation I on a surface generally oriented as follows:

$$I(\sigma,\psi) = \int \hat{n}(\sigma,\psi)\bullet\vec{\beth}(\theta,\phi)d\Omega \quad (1)$$
$$\models \sum_{i=1}^{145}\hat{n}(\sigma,\psi)\bullet\vec{\beth}_i \quad \text{(discretized sky)}$$

where $\hat{n}(\sigma,\psi)$ is the normal vector of the surface considered, σ and ψ are respectively the tilt angle and the orientation of the surface, θ and ϕ are respectively the zenith and the azimuth angle defining the position in the cumulative sky of each radiant source with a radiance value of

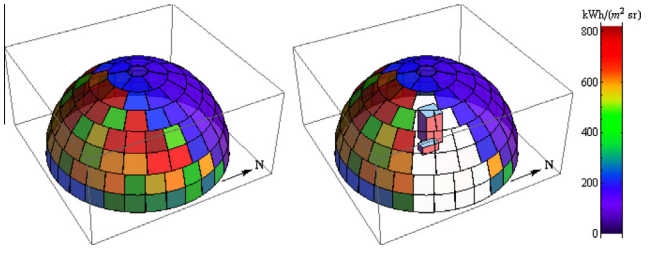

Fig. 1. Schema of the cumulative sky, simulated for Basel.

$|\vec{\beth}(\theta,\phi)|$ (W h m^{-2} s r^{-1}), in the continuous case, and $|\vec{\beth}_i|$ (W h m^{-2} s r^{-1}), in the discretized case using Tregenza patches. In particular, by definition:

$$\vec{\beth}(\theta,\phi) = \beth(\theta,\phi)\cdot\hat{n}(\theta,\phi) \quad (2)$$
$$\text{with } \hat{n}(\theta,\phi) = (\sin(\theta)\cos(\phi),\sin(\theta)\sin(\phi),\cos(\theta))$$

where we use $\hat{n}$ to indicate the direction.

In order to conduct a general proof, we consider in this section the general case of continuous normalised distributions (see Eq. (1)) and, in particular, we introduce the Banach space $\mathcal{B}$ and the space of distributions $\mathcal{D}$ defined as follows:

$$\mathcal{B} = \{\beth : [0,\pi/2]\times[0,2\pi]\to\mathbb{R}^+ \mid \beth \text{ locallyintegrable functions}\}$$
$$\text{with a positive definite scalar product } \langle\ldots|\ldots\rangle$$
$$\text{and the corresponding norm } \|\beth\| \doteq \sqrt{\langle\beth|\beth\rangle}$$
$$\mathcal{D} = \{\dot{\beth}\in\mathcal{B}| \text{ with } \|\dot{\beth}\| = 1\}$$

where we indicate the normalised distribution with a dot over the letter, with the symbol $\dot{\beth}$. Note that the following conclusions follow for all positive definite scalar products.

The radiance (not yet normalised) distribution $\beth(\theta,\phi)$ is the sum of the direct $\beth_d(\theta,\phi)$, and the diffuse $\beth_s(\theta,\phi)$, radiance distributions:

$$\beth(\theta,\phi) = \beth_d(\theta,\phi) + \beth_s(\theta,\phi) \quad (3)$$

and, in our formalism, the normalised distribution $\dot{\beth}$ has the following expression:

$$\dot{\beth} = \frac{r\dot{\beth}_d + (1-r)\dot{\beth}_s}{\|r\dot{\beth}_d + (1-r)\dot{\beth}_s\|} \quad (4)$$

where r is the ratio of the direct solar radiation contribute to the total radiation.

If we neglect infrared and ultraviolet light in the spectral radiance, the distribution $\dot{\beth}$, in general, changes because the ratio r changes and Eq. (4) assumes the following form:

$$\dot{\beth}^{(v)} = \frac{r^{(v)}\dot{\beth}_d + (1-r^{(v)})\dot{\beth}_s}{\|r^{(v)}\dot{\beth}_d + (1-r^{(v)})\dot{\beth}_s\|} \quad (5)$$

where the symbol $^{(v)}$ indicate that we are referring to the visible spectrum.

Hence, the rates r and $r^{(v)}$ are calculated by spectrum, to show that the distribution do not change appreciably. The spectrum of direct and diffuse irradiance is obtained as in Bird (1984) and Bird and Riordan (1986), on an horizontal surface. Direct irradiance for a wavelength λ (μm) at ground level can be calculated as follows:

$$\beth_{d\lambda} = H_{0\lambda}\cdot D\cdot T_{r\lambda}\cdot T_{a\lambda}\cdot T_{0\lambda}\cdot T_{w\lambda}\cdot T_{u\lambda}\cdot\cos(\theta) \quad (6)$$

where $H_{0\lambda}$ is the extraterrestrial spectral irradiance at the mean solar distance, based on the Neckel and Labs spectrum (Neckel and Labs, 1981) and tabled in Bird (1984), D is the correction factor for the earth–sun distance, θ is

the solar zenith angle, and $T_{r\lambda}$, $T_{a\lambda}$, $T_{0\lambda}$, $T_{w\lambda}$ and $T_{u\lambda}$ are the transmittance functions for Rayleigh scattering, aerosol extinction, ozone absorption, water vapour absorption, and absorption by the uniformly mixed gases (oxygen and carbon dioxide), respectively. The earth–sun distance factor D is calculated as follows (Spencer, 1971):

$$D = 1.00011 + 0.034221\cos(\varphi) + 0.00128\sin(\varphi) + 0.000719\cos(2\varphi) + 0.000077\sin(2\varphi)$$

where $\varphi = 2\pi(d-1)/365$ is the day angle, of the d^{th} day of the year. The transmittance functions is calculated as follows (Bird, 1984; Bird and Riordan, 1986):

$$T_{r,\lambda} = \exp\left[-\frac{M}{115.6406\lambda^2 - 1.335}\right],$$
$$M = \left[\cos(\theta) + 0.15(93.885-\theta)^{-1.253}\right]^{-1},$$
$$T_{a,\lambda} = \exp\left[-\beta\lambda^{\alpha}M\right],$$
$$\alpha = 1.14,$$
$$\beta = 0.075,$$
(extrapolated from results in Sakerin and Kabanov (2006))
$$T_{o,\lambda} = \exp\left[-a_{0,\lambda}O_3 M\right],$$
$$O_3 = 0.35,$$
(extrapolated from results in Leckner (1978))
$$T_{w,\lambda} = \exp\left[-0.2385\frac{a_{w,\lambda}WM}{(1+20.07a_{w,\lambda}WM)^{0.45}}\right],$$
$$W = 20,$$
(extrapolated from results in Dick etal. (2001))
$$T_{u,\lambda} = \exp\left[-1.41\frac{a_{u,\lambda}M}{(1+118.93a_{u,\lambda}M)^{0.45}}\right]$$

where $a_{0,\lambda}$, $a_{w,\lambda}$ and $a_{u,\lambda}$ are the ozone, water vapour and mixed gas absorption coefficients, respectively, and tabled in Bird (1984). Note that we assumed implicitly a pressure of 1 atm.

Diffuse irradiance for a wavelength λ (μm) at ground level can be calculated as follows:

$$\dot{\mathbb{I}}_{s\lambda} = H_{0\lambda}\cdot D\cdot T_{0\lambda}\cdot T_{w\lambda}\cdot T_{u\lambda}\cdot\cos(\theta)\cdot(.5T_{a\lambda}\cdot(1-T_{r\lambda}) + F_a W_0 T_{r\lambda}(1-T_{a\lambda})) \quad (7)$$

where $W_0 = 0.928$ is the single scattering albedo of the aerosol and $F_a = 0.82$ is the forward to total scattering ratio of the aerosol. We used the values of W_0 and F_a for the rural aerosol Bird (1984).

The solar zenith angle θ is calculated using the standard trigonometric expressions, as follows:

$$\theta = \arcsin(\sin\delta\sin L + \cos\delta\cos L\cos\omega)$$
$$\delta = 23.45\sin\left(2\pi\frac{284+d}{365}\right) \quad (8)$$

where δ is the declination calculated in the dth day of year using the Copper's formula (Cooper, 1969), L is the latitude, and ω is the hour angle. Integrating over the day with respect to ω and with a summation over the days of the year, the spectrum of the radiation cumulated in a year on an horizontal surface is calculated for Basel and Dubai, respectively, and shown in Fig. 2 for Dubai.

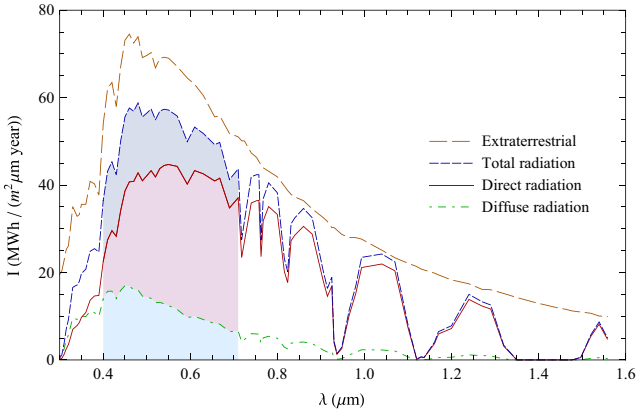

Fig. 2. Spectrum of solar extraterrestrial and at ground level radiation, cumulated in a year on an horizontal surface, in Dubai.

Using the spectra in Fig. 2, the values of the rates r and $r^{(v)}$ are calculated:

Basel	Dubai
$r^{(v)} = 0.725$	$r^{(v)} = 0.766$
$r = 0.769$	$r = 0.802$

Hence, the scalar product between $\dot{\mathbb{I}}$ and $\dot{\mathbb{I}}^{(v)}$, in Eqs. (4) and (5), is calculated to quantify the matching between these distributions, with a value from 0 to 1. It is possible to show that this scalar product has the following expression:

$$\langle\dot{\mathbb{I}}|\dot{\mathbb{I}}^{(v)}\rangle = \frac{\mathcal{F}^{r,r^{(v)}}[\langle\dot{\mathbb{I}}_d|\dot{\mathbb{I}}_s\rangle]}{\sqrt{\mathcal{F}^{r,r}[\langle\dot{\mathbb{I}}_d|\dot{\mathbb{I}}_s\rangle]\mathcal{F}^{r^{(v)},r^{(v)}}[\langle\dot{\mathbb{I}}_d|\dot{\mathbb{I}}_s\rangle]}} \quad (9)$$
$$\text{with}\quad \mathcal{F}^{a,b}[x] \doteq 1 + (2ab - a - b)(1-x)$$

Note that $|\langle\dot{\mathbb{I}}_d|\dot{\mathbb{I}}_s\rangle| \leq 1$, from the Cauchy–Schwarz inequality, and that if $\langle\dot{\mathbb{I}}_d|\dot{\mathbb{I}}_s\rangle = 1$ (i.e. they are the same distribution) then $\langle\dot{\mathbb{I}}|\dot{\mathbb{I}}^{(v)}\rangle = 1$ always.

Substituting the values of the rates obtained above and considering the worst case in which the distributions $\dot{\mathbb{I}}_d$ and $\dot{\mathbb{I}}_s$ are orthogonal, in order to have a lower-bound, we conclude that the two distributions $\dot{\mathbb{I}}$ and $\dot{\mathbb{I}}^{(v)}$ match at least to 99.75 % for Basel and 99.85 % for Dubai. Therefore we can neglect the infrared and ultraviolet, and, in particular, we can use RADIANCE on the visible spectrum to compute the irradiation on buildings.

2.3. Optimisation

The form of the building is described by relevant variables (*alleles*). The optimisation consists to find the combination of these parameters that minimises solar irradiation on the envelope. For a few different discrete variables it may be possible to exhaustively test all possibilities, but

when the parameter space to explore becomes large to very large, it is desirable to use optimisation algorithms.

With these algorithms, we should be able to find the global minimum (or minima) of a function f that depends on n independent decision variables. Put formally, the algorithm searches for the supremum (the set of variables that maximises the function) as in Eq. (10).

$$\sup\{f(\vec{x})|\vec{x} \in M \subseteq \mathbb{R}^n\} \tag{10}$$

with:

$n \in \mathbb{N}$	dimension of the problem
$f: M \to \mathbb{R}$	objective function
$M = \{\vec{x} \in \mathbb{R}^n | g_j(\vec{x}) \geqslant 0$ $\forall j \in \{1,\ldots,m\}\}, M \neq \emptyset$	feasible region
$m \in \mathbb{N}$	number of constraints

The set of inequality restrictions $g_j: \mathbb{R}^n \to \mathbb{R}$, $\forall j \in \{1,\ldots,m\}$ includes a special case of constraints due to the domain boundaries $\vec{L} \leqslant \vec{x} \leqslant \vec{H}$, with $\vec{L}, \vec{H} \in \mathbb{R}^n$. $\vec{L}$ is named the lower bound and $\vec{H}$ the upper bound of the domain.

In our case, the parameter space is defined by a geometrical characterisation of the buildings and the measure to improve is the received irradiation. For this, RADIANCE is used as a black-box.

2.4. Optimisation for energy consumption: The 'algebraic' cumulative sky

In the previous section, the annual cumulative sky has been used in order to calculate the total amount per year of solar irradiation on the envelope, as objective function. But solar irradiation is clearly counter-productive only in *warm* conditions, and not in *cold* conditions. In order to estimate the effect on the energy consumption of the AC due to solar radiation in a year, an 'algebraic' cumulative sky is reproduced, i.e. an algebraic sum in which solar radiation, at a defined hour of the year, is taken positive if the atmospheric conditions are *cold* and negative if it is *warm*.

The definition of *warm* and *cold* are here introduced ad hoc for our purpose, as a relation between the external temperature T_e and the corresponding internal comfort temperature T_c. The equation for comfort temperature in free-running buildings is almost exactly the following (Nicol and Humphreys, 2002):

$$T_c = 13.5 + 0.54 \cdot T_e \tag{11}$$

The software Meteonorm provides the external temperature and solar irradiance at each hour of the year, calculated as an average of experimental data measured in the period 1996–2005. Then the sign of the corresponding sky radiance is evaluated for each hour of the year, as shown in Fig. 3. In particular, the following definitions are introduced:

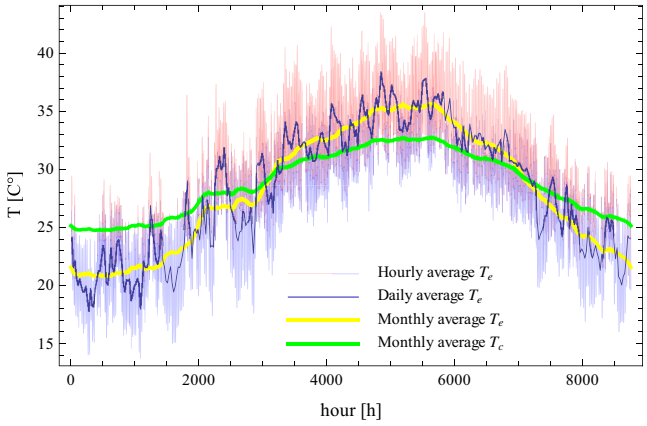

Fig. 3. Comparison between the external temperature T_e and the internal comfort temperature T_c, in Dubai.

- there are *warm* conditions, in which the sky radiance contribution are accounted for negatively if $T_e > T_c$;
- there are *cool* conditions, in which the sky radiance contribution are accounted for positively if $T_e < T_c$.

Finally the 'algebraic' cumulative sky is calculated and the optimisation of the building form is applied as above.

3. Results

The method to minimise the annual solar irradiation on the building envelope is applied to various families of possible building forms, that are defined by different parametrisations. In particular by Fourier series, Taylor series, snake form and squared form (Cubotron) respectively in Sections 3.1.1–3.1.4. In Section 3.2.1, the method is applied to the Taylor parametrisation but with different constraints, i.e. in a triangular domain.

Finally the method to minimise the annual algebraic solar irradiation is applied in order to explore the optimal forms that reduce the energy consumption of AC associated to the solar irradiation. This second method is applied to the Taylor and Cubotron parametrisation.

The results for each parametrisation used will be briefly analysed and compared in the 'Discussion' subsection.

3.1. Minimisation of the solar irradiation

First of all, we consider the problem to minimise the solar irradiation on the building's envelope. To this aim, we take into account the annual cumulative sky, as shown in Fig. 4.

3.1.1. The first parametrisation of the building's shape: Fourier series

This first case is based on an idea, already developed, of Kampf and Robinson (2010) that consists to use a two dimensional (2D) Fourier series to describe the geometry of a roof. We seek to minimise the solar irradiation

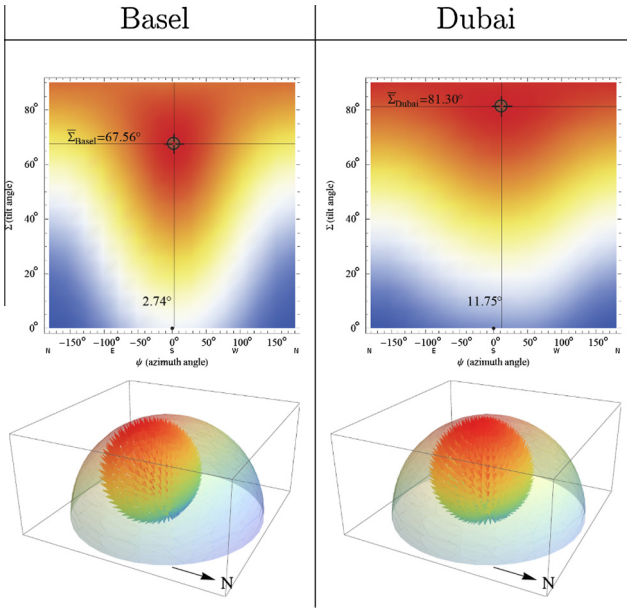

Fig. 4. Annual cumulated solar irradiation on a surface as a function of its tilt angle Σ and its orientation ψ, for Basel and Dubai.

throughout a year. For this application, the two-dimensional Fourier series, expressed in terms of sines and cosines with N and M impairs, is considered:

$$h(x,y) = \sum_{k=-(N-1)/2}^{(N-1)/2} \sum_{l=0}^{(M-1)/2} A_{kl} \cdot \cos\left(\frac{2\pi k \cdot x}{L_x(N/(N-1))} + \frac{2\pi l \cdot y}{L_y(M/(M-1))}\right) + B_{kl} \cdot \sin\left(\frac{2\pi k \cdot x}{L_x(N/(N-1))} + \frac{2\pi l \cdot y}{L_y(M/(M-1))}\right) \quad (12)$$

where $h : \mathbb{R}^2 \to \mathbb{R}$ gives the height as a function of the position (x,y) in the plane, $x \in [o, L_x], y \in [o, L_y]$, L_x and L_y delimit the domain of interest in x and y and $A_{kl}, B_{kl} \in \mathbb{R}$ are the alleles to optimise.

By definition, the function $h(x,y)$ is periodic in x and y. The period is $T_x = L_x N/(N-1)$ and $T_y = L_y M/(M-1)$ respectively for x and y. The multiplication by the factors $N/(N-1)$ and $M/(M-1)$ is introduced in order to avoid repetition in the domain of interest $x \in [o, L_x]$ and $y \in [o, L_y]$.

If Eq. (12) is derived from the Fourier series on the field $\mathbb{C}$, it can be shown that the coefficients A_{kl} and B_{kl} have the following symmetries:

$$A_{k0} = A_{-k0} \quad (13)$$

$$B_{k0} = -B_{-k0}. \quad (14)$$

Hence, the number of independent amplitudes of the sines and cosines, that are used here as parameters in the optimisation process, is equal to $N \cdot M$.

For our numerical application, the domain boundaries were chosen to be $L_x = 20$ m, $L_y = 30$ m and $N = M = 5$; giving 25 independent parameters, i.e. 25 alleles to optimise. The amplitude A_{00} is the base amplitude, which is a constant value throughout the domain. It was chosen to vary between 0 and 10 m. The other amplitudes are limited between a lower and an upper limit; in total three cases are tested:

1. $A_{kl}, B_{kl} \in [-6, 6]$ but $A_{00} \in [0, 10]$
2. $A_{kl}, B_{kl} \in [-10, 10]$ but $A_{00} \in [0, 10]$
3. $A_{kl}, B_{kl} \in [-20, 20]$ but $A_{00} \in [0, 20]$

A minimum cut value was chosen in the height of the surface at 0 m, so that when the surface goes below the ground (placed at 0 m), it is not taken into account in the irradiation calculation.

Further constraints dictate that the volume must remain within 10% of 80% of the maximum allowed which is given by a parallelepiped of 10 m by 20 m by 30 m (i.e. $10\text{ m} \cdot L_x \cdot L_y$).

Fig. 5 illustrates the results obtained with a termination criterion of 20,000 evaluations, with three different A_{max}, under the climate of Basel.

3.1.2. The second parametrisation of the building's shape: Taylor series

This second parametrisation considered consists to use a two dimensional (2D) Taylor series to describe the geometry of the roof enclosing the building's volume. Once again we seek to minimise the solar irradiation throughout a year. For this application, the two-dimensional Taylor series is expressed as follows:

$$h(x,y) = \sum_{k=0}^{N-1} \sum_{l=0}^{M-1} A_{kl} \cdot \left(\frac{x - L_x/2}{L_x}\right)^k \left(\frac{y - L_y/2}{L_y}\right)^l \quad (15)$$

where $h : \mathbb{R}^2 \to \mathbb{R}$ gives, as above, the height as a function of the position (x,y) in the plane, $x \in [o, L_x], y \in [o, L_y]$, L_x and L_y delimit the domain of interest in x and y and A_{kl} are the amplitudes. The domain boundaries were chosen to be $L_x = 20$ m, $L_y = 30$ m and $N = M = 5$. Finally the form can be tilted by an angle Σ, and, then, there are 26 alleles, that are used here as parameters in the optimisation process. Four simulations were made with constraint on the minimum volume, $V_{min} = 1000\text{ m}^3$ and $V_{min} = 4000\text{ m}^3$, and for the two cities Basel and Dubai. The coefficients are limited between a lower and an upper limit as follows:

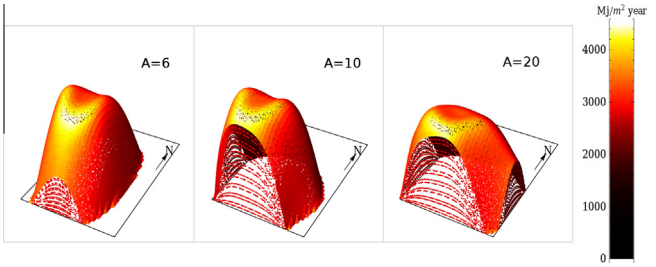

Fig. 5. Result for Fourier parametrisation after 20,000 evaluations, in 3D view, respectively for $A_{max} = 6, 10, 20$, in Basel.

$$A_{kl} \in [-200, 200] \tag{16}$$

A minimum cut value was chosen in the height of the surface at 0 m, so that when the surface goes below the ground (placed at 0 m), it is not taken into account in the irradiation calculation.

Further constraints dictate that the volume under the surface must be less than 1000 m^3, in one case, and 4000 m^3 in a second case. The simulations were made for Basel and Dubai, with a termination criterion of 10,000 evaluations, for which results are presented in Fig. 7.

3.1.3. The third parametrisation of the building's shape: Snake forms

The third parametrisation is the 'snake' type. This is obtained as a three-dimensional surface with circular sections, in general different from each other and in particular with different radius, height and transverse position of the centre. The form is defined as a continuous surface expressed by the functions $r(y) : \mathbb{R} \to \mathbb{R}, Z_c(y) : \mathbb{R} \to \mathbb{R}$ and $X_c(y) : \mathbb{R} \to \mathbb{R}$, respectively, the radius, height and position of the centre of each circular cross section along the y axis (representing the N–S direction). Each of these functions is expressed as a truncated Fourier series. As above, alleles define the amplitudes of those series.

$$\begin{aligned} Z_c(y) &= \sum_{k=0}^{4} A_k \cos\left(\frac{2\pi k \cdot y}{L_y(N/(N-1))}\right) \\ &\quad + A_{k+4} \sin\left(\frac{2\pi k \cdot y}{L_y(N/(N-1))}\right), \\ X(y) &= L_x/2 + \sum_{k=0}^{3} A_{k+9} \cos\left(\frac{2\pi k \cdot y}{L_y(N/(N-1))}\right) \\ &\quad + A_{k+12} \sin\left(\frac{2\pi k \cdot y}{L_y(N/(N-1))}\right), \\ r(y) &= \sum_{k=0}^{4} |A_{k+16}| + A_{k+16} \cos\left(\frac{2\pi k \cdot y}{L_y(N/(N-1))}\right) \\ &\quad + A_{k+20} + |A_{k+20}| \sin\left(\frac{2\pi k \cdot y}{L_y(N/(N-1))}\right) \end{aligned} \tag{17}$$

where A_k with $k = 0, \ldots, 24$ are 25 independent parameters. Finally the form can be tilted by an angle Σ, and, then, there are 26 alleles, that are used here as parameters in the optimisation process. As in the previous cases, the domain boundaries were chosen to be $L_x = 20$ m and $L_y = 30$ m. Four simulations are made with constraint on the minimum volume, $V_{min} = 1000$ m^3 and $V_{min} = 4000$ m^3, and for the two cities Basel and Dubai. The optimal solutions obtained, with a termination criterion of 15,000 evaluations, are shown in Fig. 7.

3.1.4. The fourth parametrisation of the building's shape: Cubotron (squared form)

The fourth parametrisation introduced is closer to the more common constructions, with squared form. In particular, the form is defined by a three floor building, each 3 m high, with a fixed gross floor area equal to 400 m^2 and vertical walls. Each floor has a shape defined by orthogonal straight lines, in particular, as shown in Fig. 6 the form can change by moving the point B along the curve 1, and the point D along the curve 2, i.e. the two linear positions of B and D along the curves 1 and 2 define the form to be square-, 'L'- or 'S'-shape, i.e. two alleles for each floor. The curve 1 and 2 are defined in order to maintain the surface of the floor fixed. Other six parameters (two for each floor) define the deformation by homothetic transformation of the floors, but the gross floor area of the building is maintained fixed, i.e. five independent alleles. Moreover each floor may have a general orientation, defined by an angle, i.e. three alleles for the three floors. Finally the position of the ground floor is fixed and the ones on the other two floors may translate horizontally, i.e. four alleles. The form of the building is then defined by 18 alleles.

The optimal solutions obtained, with a termination criterion of 20,000 evaluations, are shown in Fig. 7. The interesting aspect of this case is that a realistic squared building follows the trend of the optimal forms previously obtained.

3.1.5. The fifth parametrisation of the building's shape: Triangular domain

This simulation is implemented to verify if the form depends on the geometrical form of the site, that is a geometrical constraint of the problem. The Taylor parametrisation is used, as described in details in Section 3.1.2 but in a triangular domain, rather than the rectangular domain previously used. This domain is represented by an equilateral triangle with the same area as the domain in Section 3.1.2 (i.e. with the common length of the sides = 37.22 m), and it is oriented as shown in Fig. 7d.

The results, with a termination criterion of 10,000 evaluations, are show in Fig. 7.

3.2. Minimisation of the energy consumption by the use of the "algebraic" cumulative sky

In this section, we apply the optimisation algorithm to reduce the annual energy consumption of the AC due to the solar irradiation on the building's envelope. To achieve that aim, we use the algebraic cumulative sky in order to compute the annual useful incident solar irradiation on

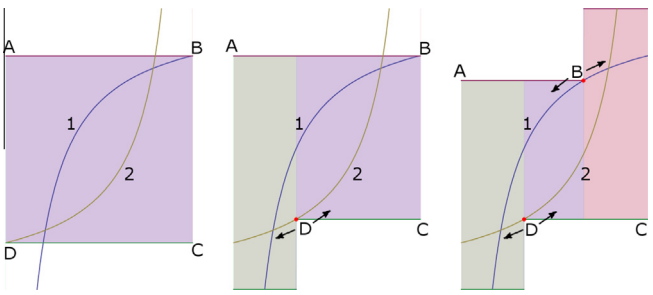

Fig. 6. Possible squared form of the floors.

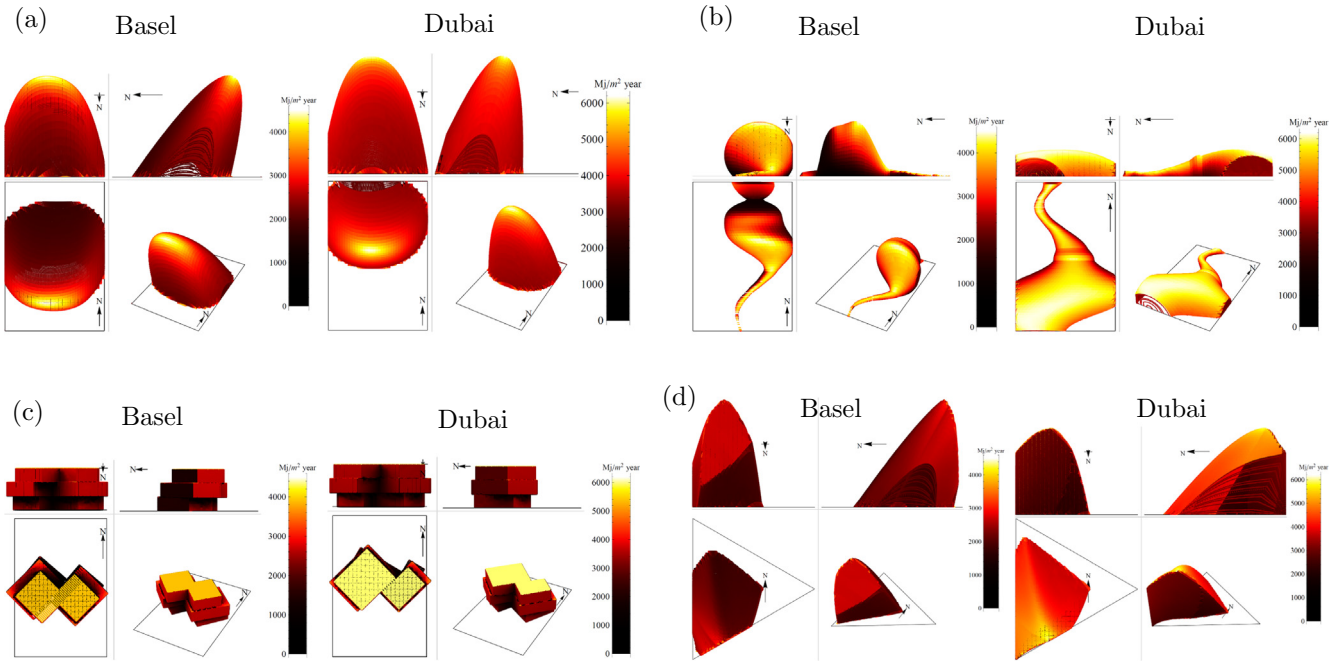

Fig. 7. Result for Taylor (a), Snake (b), Cubotron (c) parametrisations and Taylor parametrisation in triangular domain (d), in 3D view, respectively for Basel (left) and Dubai (right).

the building envelope. The method consists in using weather data to define in which case the solar irradiation on the envelope gives a positive or negative contribution depending on the external temperature in order to maintain internal comfort of the occupants. The contribution is further associated to the data of the solar irradiation for each hour of a typical year. The algebraic cumulative sky constructed on that basis has the advantage to present particular zones where the solar radiation is useful all year long.

The algebraic cumulative skies in Basel and Dubai are shown in Fig. 8.

3.2.1. Taylor parametrisation

The Taylor parametrisation, described in Section 3.1.2, is the first one chosen in order to find the optimal form for the second problem, i.e. to minimise the air-conditioning needs due to solar radiation, with the algebraic cumulative sky. Indeed, in the previous sections the Taylor parametrisation seems to have the best performance, i.e. the minimum fitness value for a fixed number of evaluations.

The results, with a termination criterion of 15,000 evaluations, are shown in Fig. 9. Even in this case the optimal form is compact, but oriented to the south-west. The reason could be that in the morning the external temperature T_e is lower than in the afternoon. Hence, solar radiation tends to give a positive contribute in the morning, but a negative contribute in the afternoon.

3.2.2. Cubotron parametrisation

The second parametrisation chosen to explore the optimal form that minimise the annual energy consumption is

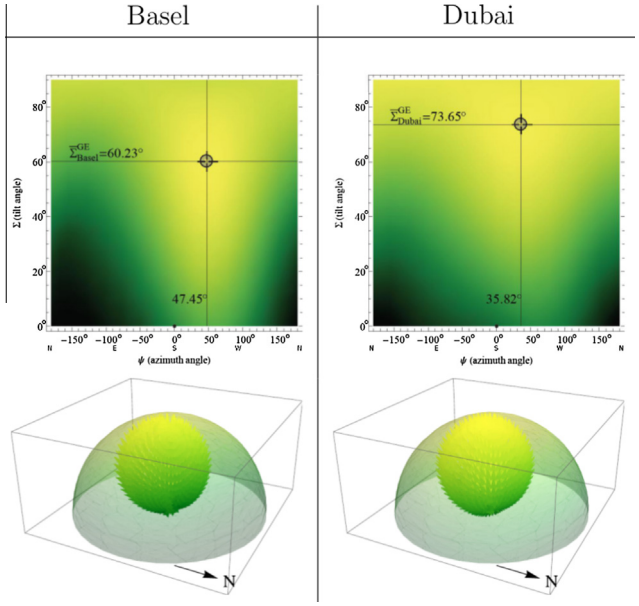

Fig. 8. Annual 'algebraic' cumulated solar radiation on a surface as a function of its tilt angle Σ and its orientation ψ, for Basel and Dubai.

the 'cubotron' parametrisation, previously described in detail in Section 3.1.4. In fact, this parametrisation is close to typical building forms in construction industry, and then useful for a more practical context. The results, with a termination criterion of 20,000 evaluations, are shown in Fig. 9.

3.3. Discussion

Two different optimisation problems have been considered, respectively to minimise the annual cumulative and

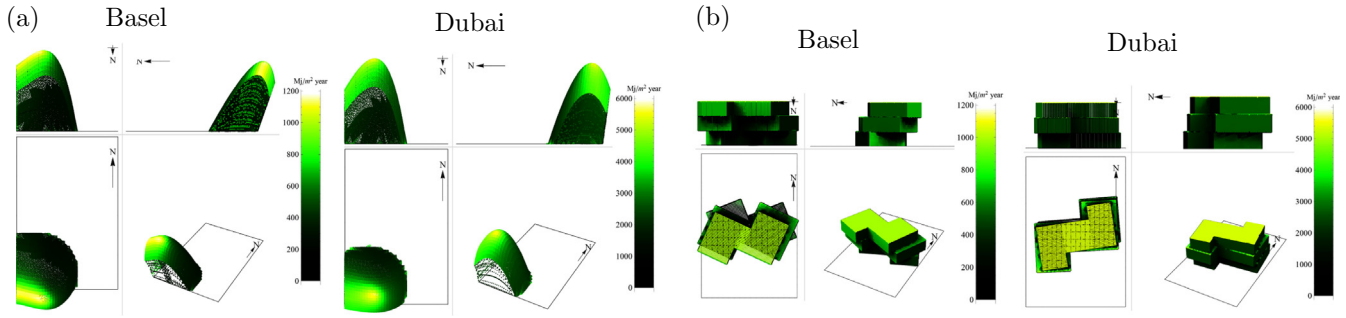

Fig. 9. Optimal form of the Taylor and Cubotron parametrisation to reduce energy consumption due to solar radiation, with $V_{min} = 1200\ m^3$, in 3D view, respectively for Basel and Dubai.

algebraic solar irradiation on the building's envelope. In both cases, the Taylor parametrisation achieves the best performance. Results has been obtained after 10,000 up to 20,000 evaluations. Fig. 10 shows the evolution of the fitness (annual solar irradiation) of the candidates along with the evaluations of the Taylor parametrisation made in the HDE part of the evolutionary algorithm.

The results obtained show that the optimal forms usually take a compact form oriented to a particular direction in the sky that depends on the site, to minimise whether solar irradiation or air-conditioning needs. In Fig. 4, the (annual cumulated) solar irradiation on a surface is calculated as a function of its tilt angle Σ and orientation ψ, for Basel and Dubai. In this Figure we can identify a particular point that represents the point of maximum cumulated solar irradiation. In other words, a flat surface should be orthogonal to (i.e. oriented to) this direction in order to collect the highest amount of solar irradiation cumulated in a year. Similarly, in Fig. 8 we can identify the point of maximum algebraic solar irradiation (MASI). It is interesting to make a comparison between the orientation of the optimal forms of both problems and the direction in the sky of the points of the maximum cumulated and algebraic solar irradiation respectively, as shown in Fig. 11. In particular the tilt angle Σ of the optimal forms minimising solar irradiation tends to be close to the altitude angle $\bar{\Sigma}$ of the point of maximum cumulated solar irradiation, as shown in Table 1. Likewise, the optimal forms minimising the air-conditioning needs have Σ close to the altitude angle of the maximum algebraic solar irradiation $\bar{\Sigma}_a$, as shown in Table 2.

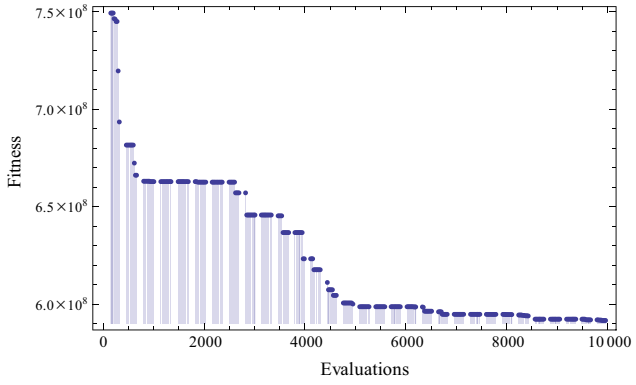

Fig. 10. The fitness (solar irradiation) evolution within the evolutionary sub-algorithm HDE for the Taylor parametrisation.

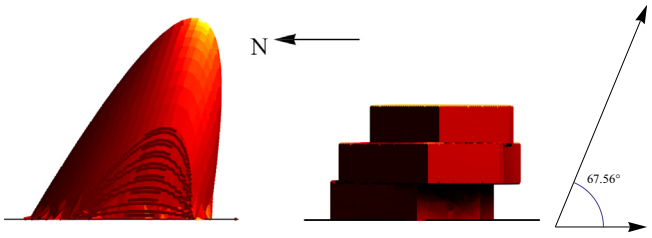

Fig. 11. The optimal forms inclined in the direction of maximum radiation.

Table 1
Results of optimisation of the building form to reduce solar irradiation, in Basel and Dubai. The altitude angle of the point of maximum cumulated solar irradiation $\bar{\Sigma}$ is shown in brackets.

Parametrisation	V (m^3)	Σ(67.56°)	Φ_{sol} (W h/year)
Basel			
Taylor $V_{min} = 1000$ m^3	1001.03	71.28°	$2.40 \cdot 10^8$
Snake $V_{min} = 1000$ m^3	1000.74	90.98°	$2.59 \cdot 10^8$
Triangle $V_{min} = 1000$ m^3	1000.18	50.39°	$2.71 \cdot 10^8$
Taylor $V_{min} = 4000$ m^3	4001.30	65.50°	$5.92 \cdot 10^8$
Snake $V_{min} = 4000$ m^3	4000.89	90.79°	$6.57 \cdot 10^8$
Triangle $V_{min} = 4000$ m^3	4001.09	60.76°	$6.62 \cdot 10^8$
Cubotron	1200	–	$2.99 \cdot 10^8$
Parametrisation	V (m^3)	Σ(81.30°)	Φ_{sol} (W h/year)
Dubai			
Taylor $V_{min} = 1000$ m^3	1000.28	81.22°	$3.82 \cdot 10^8$
Snake $V_{min} = 1000$ m^3	1000.07	92.92°	$5.08 \cdot 10^8$
Triangle $V_{min} = 1000$ m^3	1000.36	77.26°	$3.82 \cdot 10^8$
Taylor $V_{min} = 4000$ m^3	4005.15	74.13°	$9.36 \cdot 10^8$
Snake $V_{min} = 4000$ m^3	4000.10	90.06°	$10.58 \cdot 10^8$
Triangle $V_{min} = 4000$ m^3	4004.12	59.41°	$11.12 \cdot 10^8$
Cubotron	1200	–	$4.68 \cdot 10^8$

Moreover, the direction of maximum 'algebraic' irradiation is not in the south but in the south-west direction, due to the fact that in the morning the external temperature T_e is lower than in the afternoon. Hence, solar radiation tends

Table 2
Results of optimal forms of Taylor and Cubotron parametrisation to reduce energy consumption, in Basel and Dubai. The altitude angle of the MASI point $\bar{\Sigma}_a$ is shown in brackets.

Parametrisation	V (m^3)	$\Sigma(60.23°)$	Φ_{sol} (W h/year)
Basel			
Taylor $V_{min} = 1200$ m^3	1204.58	70.44°	$0.57 \cdot 10^8$
Cubotron	1200	–	$0.65 \cdot 10^8$
Parametrisation	V (m^3)	$\Sigma(73.65°)$	Φ_{sol} (W h/year)
Dubai			
Taylor $V_{min} = 1200$ m^3	1203.56	82.11°	$2.97 \cdot 10^8$
Cubotron	1200	–	$3.33 \cdot 10^8$

to give a positive contribution in the morning, but a negative contribution in the afternoon.

4. Conclusions

In this paper, we use the hybrid evolutionary algorithm CMA-ES/HDE in order to find the optimal building form that minimise the annual cumulative solar irradiation on the building's envelope. Then, the same method is used for a second problem, i.e. to minimise the air-conditioning needs by considering the algebraic contribution of solar irradiation on the building's envelope with respect to the external temperature. In both problems we find similar conclusions as follows:

- reasonable and stable optimal forms are obtained after 10,000 up to 20,000 evaluations with a number of variables (alleles) between 18 and 26;
- the Taylor parametrisation leads to the best candidates;
- the optimal forms are compact and oriented to a particular direction in the sky that depends on the site, following a sort of self-shading concept;
- the optimal forms 'avoid' the point of maximum (cumulated or algebraic) solar irradiation in order to reduce the annual (cumulated or algebraic) solar irradiation;
- the optimal forms 'avoid' the direct irradiation, since the points of maximum solar irradiation are close to the sun's path, reducing the need of using shading systems on the building's envelope;
- the MASI point is usually in the south-west direction.

Briefly, a building designer should design the form of the building's envelope as compact as possible with respect to the direction of maximum annual solar irradiation of the site considered, that is a well known direction for photovoltaic applications, following the self-shading concept. In the case of a more complicated problem when minimising the annual air-conditioning needs of the building, the evolution of the external temperature in each hour of the day along all the year should be analysed in order to calculate the position of the MASI point. However, in the scenarios considered we find that this point is usually in the south-west direction, with a lower altitude angle with respect the well know point of maximum cumulated solar irradiation.

Acknowledgment

We thank the Solar Energy and Building Physics Laboratory (LESO-PB) of the École Polytechnique Fédérale de Lausanne (EPFL) for the computing resources provided for this work.

Appendix A.

Demonstration of Eq. (4): $\dot{\mathbb{J}} = \frac{r\dot{\mathbb{J}}_d + (1-r)\dot{\mathbb{J}}_s}{\|r\dot{\mathbb{J}}_d + (1-r)\dot{\mathbb{J}}_s\|}$

$$\begin{aligned}\dot{\mathbb{J}} &= \frac{\mathbb{J}}{\|\mathbb{J}\|} = \frac{\mathbb{J}_d + \mathbb{J}_s}{\|\mathbb{J}_d + \mathbb{J}_s\|} = \frac{\|\mathbb{J}_d\|}{\|\mathbb{J}_d + \mathbb{J}_s\|}\dot{\mathbb{J}}_d + \frac{\|\mathbb{J}_s\|}{\|\mathbb{J}_d + \mathbb{J}_s\|}\dot{\mathbb{J}}_s \\ &= \alpha\left(r\dot{\mathbb{J}}_d + (1-r)\dot{\mathbb{J}}_s\right) \in \mathcal{B} \end{aligned} \tag{18}$$

where $r = \frac{\|\mathbb{J}_d\|}{\|\mathbb{J}_d\| + \|\mathbb{J}_s\|}$ and $\alpha = \frac{\|\mathbb{J}_d\| + \|\mathbb{J}_s\|}{\|\mathbb{J}_d + \mathbb{J}_s\|}$.

Finally the expression (18) and $\frac{r\dot{\mathbb{J}}_d + (1-r)\dot{\mathbb{J}}_s}{\|r\dot{\mathbb{J}}_d + (1-r)\dot{\mathbb{J}}_s\|} \in \mathcal{B}$ are two elements of the Banach (linear) space $\mathcal{B}$, differing only by a scalar factor. However those two elements are both normalised. Therefore they must be the same element. In particular:

$$\dot{\mathbb{J}} = \alpha\left(r\dot{\mathbb{J}}_d + (1-r)\dot{\mathbb{J}}_s\right) = \frac{r\dot{\mathbb{J}}_d + (1-r)\dot{\mathbb{J}}_s}{\|r\dot{\mathbb{J}}_d + (1-r)\dot{\mathbb{J}}_s\|} \quad \square$$

Demonstration of Eq. (9):

$$\begin{aligned}\langle\dot{\mathbb{J}}|\dot{\mathbb{J}}^{(v)}\rangle &= \left\langle \frac{r\dot{\mathbb{J}}_d + (1-r)\dot{\mathbb{J}}_s}{\|r\dot{\mathbb{J}}_d + (1-r)\dot{\mathbb{J}}_s\|} \middle| \frac{r^{(v)}\dot{\mathbb{J}}_d + (1-r^{(v)})\dot{\mathbb{J}}_s}{\|r^{(v)}\dot{\mathbb{J}}_d + (1-r^{(v)})\dot{\mathbb{J}}_s\|} \right\rangle \\ &= \frac{\langle r\dot{\mathbb{J}}_d + (1-r)\dot{\mathbb{J}}_s | r^{(v)}\dot{\mathbb{J}}_d + (1-r^{(v)})\dot{\mathbb{J}}_s\rangle}{\|r\dot{\mathbb{J}}_d + (1-r)\dot{\mathbb{J}}_s\|\|r^{(v)}\dot{\mathbb{J}}_d + (1-r^{(v)})\dot{\mathbb{J}}_s\|}\end{aligned}$$

Therefore, we obtain the following expression, since $\|\mathbb{J}\| \doteq \sqrt{\langle\mathbb{J}|\mathbb{J}\rangle}$:

$$\langle\dot{\mathbb{J}}|\dot{\mathbb{J}}^{(v)}\rangle = \frac{F^{r,r^{(v)}}[\dot{\mathbb{J}}_d, \dot{\mathbb{J}}_s]}{\sqrt{F^{r,r}[\dot{\mathbb{J}}_d, \dot{\mathbb{J}}_s]}\sqrt{F^{r^{(v)},r^{(v)}}[\dot{\mathbb{J}}_d, \dot{\mathbb{J}}_s]}}$$

where $F^{a,b}[x,y] \doteq \langle ax + (1-a)y | bx + (1-b)y\rangle$. However, $\dot{\mathbb{J}}_d$ and $\dot{\mathbb{J}}_s$are normalised, so we obtain the following expression for F:

$$\begin{aligned}F^{a,b}[\dot{\mathbb{J}}_d, \dot{\mathbb{J}}_s] &= \langle a\dot{\mathbb{J}}_d + (1-a)\dot{\mathbb{J}}_s | b\dot{\mathbb{J}}_d + (1-b)\dot{\mathbb{J}}_s\rangle \\ &= ab\langle\dot{\mathbb{J}}_d|\dot{\mathbb{J}}_d\rangle + (a(1-b) + b(1-a))\langle\dot{\mathbb{J}}_d|\dot{\mathbb{J}}_s\rangle \\ &+ (1-a)(1-b)\langle\dot{\mathbb{J}}_s\dot{\mathbb{J}}_s\rangle = 1 + 2ab - a - b \\ &+ (a+b-2ab)\langle\dot{\mathbb{J}}_d|\dot{\mathbb{J}}_s\rangle = 1 + (2ab - a - b) \\ &(1 - \langle\dot{\mathbb{J}}_d|\dot{\mathbb{J}}_s\rangle) \doteq \mathcal{F}^{a,b}[\langle\dot{\mathbb{J}}_d|\dot{\mathbb{J}}_s\rangle]\end{aligned}$$

where $\mathcal{F}^{a,b}[x] \doteq 1 + (2ab - a - b)(1-x)$. Finally Eq. (9) follows by substitution.

References

Bird, R.E., 1984. A simple, solar spectral model for direct-normal and diffuse horizontal irradiance. Sol. Energy 32 (4), 461–471.

Bird, R.E., Riordan, C., 1986. Simple solar spectral model for direct and diffuse irradiance on horizontal and tilted planes at the earth's surface for cloudless atmospheres. J. Appl. Meteorol. 25, 87–97.

Caruso, G., Fantozzi, F., Leccese, F., 2013. Optimal theoretical building form to minimize direct solar irradiation. Sol. Energy 97, 128–137.

Cooper, P.I., 1969. The absorption of radiation in solar stills. Sol. Energy 12 (3), 333–346.

Dick, Galina, Gendt, Gerd, Reigber, Christoph, 2001. First experience with near real-time water vapor estimation in a German GPS network. J. Atmos. Solar Terr. Phys. 63 (12), 1295–1304.

Farmani, R., Wright, J.A., Loosemore, H.A., 2002. Optimization of building thermal design and control by multi-criterion genetic algorithm. Energy Build. 34, 959–972.

Jedrzejuk, H., Marks, W., 2002. Discrete polyoptimization of energy-saving building. Arch. Civ. Eng. 48, 331–347.

Kampf, J.H., Robinson, D., 2009. A hybrid CMA-ES and HDE optimisation algorithm with application to solar energy potential. Appl. Soft Comput. 9 (2), 738–745.

Kampf, J.H., Robinson, D., 2010. Optimisation of building form for solar energy utilisation using constrained evolutionary algorithms. Energy Build. 42 (6), 807–814.

Kampf, J.H., Montavon, M., Bunyesc, J., Bolliger, R., Robinson, D., 2010. Optimisation of buildings' solar irradiation availability. Sol. Energy 84 (2), 596–603.

Larson, G.W., Shakespeare, R.A., 1998. Rendering with Radiance. Morgan Kaufman Publishers.

Leckner, B., 1978. The spectral distribution of solar radiation at the earth's surface-elements of a model. Sol. Energy 20 (2), 143–150.

Marks, W., 1997. Multicriteria optimisation of shape of energy-saving buildings. Build. Environ. 32, 331–339.

Neckel, Heinz, Labs, Dietrich, 1981. Improved data of solar spectral irradiance from 0.33 to 1.25μ. Sol. Phys. 74, 231–249.

Nicol, J.F., Humphreys, M.A., 2002. Adaptive thermal comfort and sustainable thermal standards for buildings. Energy Build. 34, 563–572.

Rivard, H., Wang, W., Zmeureanu, R., 2006. Floor shape optimization for green building design. Adv. Eng. Inform. 20, 363–378.

Robinson, D., Stone, A., 2004. Irradiation modelling made simple: the cumulative sky approach and its applications. In: Plea2004, Eindhoven, The Netherlands, 2004.

Sakerin, S.M., Kabanov, D.M., 2006. Spectral dependences of the atmospheric aerosol optical depth in the extended spectral region of 0.4–4 μm. In: Sixteenth ARM Science Team Meeting Proceedings, March 27–31, 2006. Albuquerque, NM, USA.

Spencer, J.W., 1971. Fourier series representation of the position of the sun. Search 2, 172.

Terna s.p.a. Previsioni della domanda elettrica in italia e del fabbisogno di potenza necessario. <http://www.terna.it/linkclick.aspx?fileticket=103363>.

Tuhus-Dubrow, D., Krarti, M., 2010. Genetic-algorithm based approach to optimise building envelope design for residential buildings. Build. Environ. 45, 1574–1581.

Yi, Y.K., Malkawi, A., 2009. Optimizing building form for energy performance based on hierarchical geometry relation. Autom. Constr. 18, 825–833.